



Impact of Stochastic Load and Hybrid Distributed Generation Penetration Level on Transient Stability of Power Systems

P. K. Olulope^{1*} and K. A. Folly²

¹*Department of Electronic and Electrical Engineering, Ekiti State University (EKSU), Ado Ekiti, Nigeria.*

²*Department of Electrical Engineering, University of Cape Town, South Africa.*

Authors' contributions

This work was carried out in collaboration between authors PKO and KAF. Both authors read and approved the final manuscript.

Article Information

DOI: 10.9734/BJAST/2016/28163

Editor(s):

(1) Rodolfo Dufo López, Electrical Engineering Department, University of Zaragoza, Spain.

Reviewers:

(1) Yonghui Sun, College of Energy and Electrical Engineering, Hohai University, China.

(2) Peng Zeng, Chinese Academy of Sciences, China.

(3) Jun Yang, Wuhan University, China.

(4) Yajing Gao, North China Electric Power University, China.

(5) Mir Sayed Shah Danish, University of the Ryukyus, Japan.

Complete Peer review History: <http://www.sciencedomain.org/review-history/17297>

Original Research Article

Received 4th July 2016
Accepted 13th November 2016
Published 21st December 2016

ABSTRACT

The deployment and integration of hybrid power system into the distribution network is increasing because of the potential to provide higher quality and more reliable power to consumer than a system based on a single source. The combination of two or more energy sources and its integration into the distribution network coupled with the varying load introduce different dynamics into the system than the system with single source. The impact of stochastic load and increasing penetration of hybrid distributed generation on transient stability is presented in this paper. To investigate this impact, a detail modelling of grid connected hybrid wind/solar PV and small hydropower system with a single machine infinite system is carried out. The configuration of the proposed grid connected hybrid distributed generation (HDG) consists of a doubly-fed induction generator (DFIG), a solar PV and a small hydropower system (SHP) connected together. The wind

*Corresponding author: E-mail: paulade001@yahoo.com;

turbine is integrated through PWM converter into the existing grid while the solar PV consists of DC sources integrated through PWM inverter and the hydro power is directly connected using a synchronous generator. The simulations were performed in DlgSILENT power factory software.

Keywords: Hybrid distributed generation; stochastic load critical clearing time; wind turbine; Solar PV; hydropower system; based load; additional load.

1. INTRODUCTION

The deployment of hybrid power system into the distribution network is increasing due to its potential to provide quality and reliable power [1]. When it is used as distributed generator, i.e., connected to the distribution system in a horizontally integrated market, it provides voltage control and improved voltage profile. However, the objective of providing good stability when a three-phase fault occurred will not be realized without detail transient stability analysis of HDG. This is because some energy sources are weather dependent (e.g. Solar PV and Wind power) and the dynamics associated with transient stability when HDG is used are completely different from the single energy source. These diversities in the dynamics contribute to the complexities of the network and make the system prone to serious instabilities which can result into blackout. Furthermore, when these generators are connected to the distribution network which was not originally designed for bi-directional power flow, it produces further complexities and increases the possibilities of instabilities. Hybrid distributed generation with multisource therefore can be defined as a small set of co-operating units generating electricity and heat, with diversified primary energy carriers (renewable and non-renewable), which are located closed to the consumers end. The coordination of their operations takes place by utilizing advanced power electronics [2]. They are either grid connected or standalone systems, renewable or non-renewable systems [2]. Currently, there is wide-spread use of distributed generation across the globe though the level of penetration is still low [3]. By year 2020, the penetration level of DG in some countries such as USA is expected to increase by 25% as more independent power producers; consumers and utility companies imbibe the idea of distributed generation [3]. The rapid progress in renewable energy power generation technologies and the awareness of environmental protection have been the major reasons why alternative energy and distributed generation is a promising area [4].

Because some of renewable energy sources can complement each other, multi-source alternative energy systems have great potential to provide higher quality and more reliable power to consumers than a system based on a single source [5-6]. The larger the penetration level of hybrid distributed generation (HDG) in a power system, the more difficult it becomes to predict, to model, to analyse and to control the behaviour of such system [5]. There are many reasons why integration of HDG should be investigated. Some of which are:

1. The variability of the hybrid energy sources causes instability to the grid in a way that is different from the single energy source.
2. Since the DG complements one another, the outputs are also interdependent resulting in possibilities of higher degree of instabilities compare to a single energy source.
3. Some HDGs using induction generators are not grid friendly because they consume reactive power instead of generating it. So when this generator is combined with other renewable energies e.g. solar PV, there is tendency of higher degree of instability
4. Most power converters do not have adequate control mechanism to actively support DG and HDG integration.
5. Also, existing protection mechanism might not be able to take care of the problem of bi-directional power flow that takes place due to DG connection in radial networks.
6. New design controllers are needed to effectively manage the multi-energy sources distributed generation in order to service remote villages.
7. Possibilities of insufficient supply will be higher in a location where Solar PV alone or Solar PV combined with other renewable energies because PV does not supply energy during the nights.
8. Lack of inertia constant contributes to the poor voltage regulation and the low power

quality produce by PV arrays. It therefore increases instability during fault [7].

9. Most renewable energies are weather dependent with constant daily load variation leading to negative impact on the entire system [5].

During varying load condition, the load cannot be sustained under seasonal changes and the natural intermittent properties of wind and solar PV. As a result, energy storage system is required in order to properly manage the system. In grid connected HDG, the grid provides the energy support that enhances the system energy management and possibly the stability of the system.

However, the stability of the system is influenced by load variation coupled with intermittency of the energy sources and high penetration level of HDG. These configurations among many other things need to be investigated to understand the interactions between the hybrid distributed generation and the grid.

The research studies already published in this area are mostly on the deployment and integration of single source energy system [7-14]. Ref [13] investigated the impact of high penetration of DG on transient stability. The DGs considered in the case study are synchronous and asynchronous generators. It is found that DG influences the system transient stability differently depending on DG penetration levels, DG grid connection strength, different DG technologies, and DG protection schemes. Reference [14] investigated the impact of high penetration of Solar PV on the transient stability. Several other papers reported the poor dynamic state of the system as the penetration level increases. Also, several hybrid power systems have been developed [15-16]. An isolated network for very low voltage decentralized energy production and storage based on photovoltaic and wind was developed, mainly considering the energy management and control of the photovoltaic and wind hybrid system [17]. A grid connected hybrid scheme for residential power supply based on an integrated PV array and a wind-driven induction generator were discussed [18,19]. Hybrid power systems based on steady state, unit sizing, optimization techniques in other to extract maximum power from the hybrid system and standalone have been well researched. However, none of the papers reviewed above mentioned transient state and none also considered additional energy

sources such as small hydropower system. Most of the papers did not consider the integration of HDG into the distribution system. Rather, HDG was connected into the transmission system. Interactions of HDG with the grid, effect of additional power transmitted across distribution corridor on transient stability, unexpected fault, bi-directional power flow from Hybrid DG, electromechanical oscillations due to system with different inertia constant, torsional interactions of wind turbine with power system control and grid are some of the new things to investigate for effective integration of HDG in other to prevent the future grid from any unexpected cascaded events. Others issues are stochastic load and its effect on the HDG. This study investigates the dynamic impact of stochastic load and penetration level of hybrid Wind/Solar PV/small Hydro power on transient stability. To investigate this impact, the modelling of grid connected wind / PV/small hydro power with a single machine infinite system is carried out in DigSILENT power factory. The configuration of the proposed grid connected hybrid distributed generation (HDG) consists of variable speed Wind turbine with doubly-fed induction generator (DFIG), Solar PV and small hydro power. The wind turbine is integrated through PWM converter into the existing grid while the solar PV incorporated into the system consists of DC sources integrated through PWM inverter. The small hydropower system is modelled as synchronous generator.

The rest of the paper is organized as follows: Section 2 summarizes distributed generation and hybrid distributed generation concepts while section 3 gives the mathematical modelling of HDG. Section 4 describes the arrangement of the proposed configuration and the transient stability indicator. Section 5 presents the simulation and section 6 discusses the results. Conclusion is described in section 7.

2. DISTRIBUTED GENERATION AND HYBRID DISTRIBUTED GENERATION CONCEPT

Small generators connected to the distributed network in other to service the consumer load is called distributed generation. Also, a large wind farm connected to the network to meet consumer demand is also assumed to be distributed generation. Presently, the promising sources of distributed generation are wind turbine and Solar PV. A Solar PV harvests energy directly from sunlight and converts it to electricity. Due to the

high initial cost, the number of customer involved in the usage of solar PV is still low. Later, as the cost of PV began to decrease, there will be an increasing usage across the globe and several other applications will be developed [7]. However, the low running cost and the maintenance cost of these Solar PVs as well as

the long life usage make it an attractive alternative energy source.

Also, wind turbine especially the doubly-fed induction generator has the ability to provide supplementary active and reactive power to the existing grid.

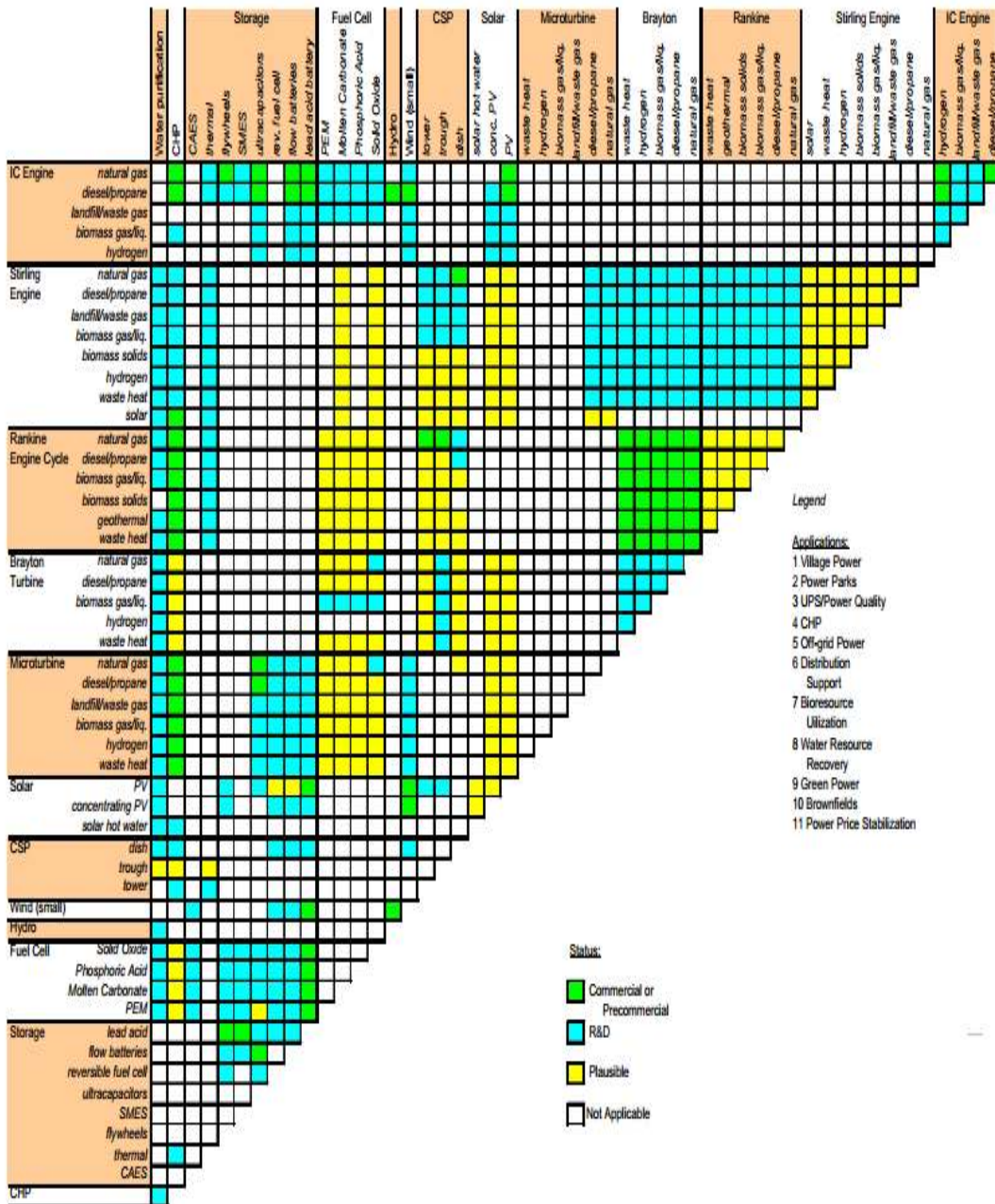


Fig. 1. Matrix describing the hybrid distributed generation [7]

DFIG converts energy inherent in wind to electricity through wind turbine, shaft, induction generator and various controllers to ensure proper grid integration and friendliness. Like solar PV, wind output power depends on the availability of wind.

Many of the primary energy sources are complimentary and abundant in nature which gives it a good opportunity to increase availability, power quality and flexibility of power supply when they are fully optimized. The objective of the integration is to capitalize on the strengths of both conventional and renewable energy sources, both cogeneration and non-cogeneration types. The combination of hybrid power generation was represented in matrix form in ref [7] and is shown in Fig. 1. Fig. 2 shows a simplified configuration of the proposed hybrid distributed generation. Three scenarios are mentioned in this paper namely the import mode, the balanced mode and the export mode, but only the export mode is analysed. The export mode is shown in Fig. 2 and it describes how the load is supplied by the centralized generator and the distributed generator. The modes are further explained below:

Import mode: In this mode, the load demands are supplied by GEN2 and HDG with additional supply from the GRID.

Balanced mode: In this mode, the load demands are met by the combination of GEN2 and HDG without any extra supply from the GRID. This means that the power generated by HDG and GEN 2 is sufficient to meet the load demands.

Export mode: In this mode, HDG and GEN2 supply the loads and export the excess generation to the GRID. This is shown in Fig. 2.

The penetration level for HDG is defined as:

$$\% PL_{HDG} = \frac{P_{HDG}}{P_{HDG} + P_{CG}} \times 100 \quad (1)$$

where $\%PL_{HDG}$ is the percentage penetration of the DG/HDG, P_{HDG} is the active power generated by HDG and P_{CG} is the active power from the centralized generators (GRID and GEN2).

$$P_{CG} + P_{HDG} = P_{LOAD}$$

where P_{LOAD} is the power delivered to the load

In all the simulations, the active and the reactive power of GEN2 are kept constant.

3. MODELLING OF HYBRID DISTRIBUTED GENERATION

3.1 Modelling Doubly-fed Induction Generator (DFIG) For Stability Studies

DFIG is widely preferred as the electrical generator for a wind turbine because it is easy to control and its robustness [20]. DFIG is a wound rotor induction generator with voltage source converter connected to the slip-rings of the rotor. DFIG interacts with the grid through the rotor and stator terminal. The induction generator is connected to the grid through the stator terminals, but the rotor terminals are connected to the grid via a partial-load variable frequency AC/DC/AC converter (VFC) [21] as shown in Fig. 3.

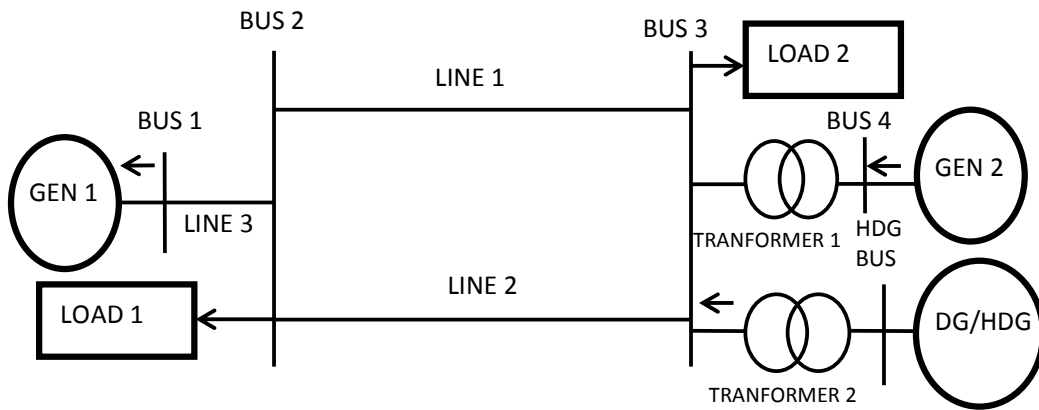


Fig. 2. Proposed modeling configuration for export mode

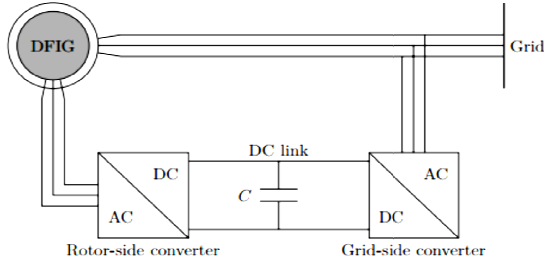


Fig. 3. DFIG with its converter [21]

To represent induction machine under system disturbance, it is desirable to use a double-cage model which represents transient and sub transient behaviour of the machine accurately [22-25]. For modelling the DFIG converters, it is assumed that the converters are ideal and the DC link voltage between the converters is constant. The rotor side converter is connected to the rotor of DFIG via brushes while the grid-side converter is connected to the grid. A capacitor is connected between the converters that act as DC voltage source. The DC voltage source decouples the rotor side converter from the grid-side converter. The rotor side converter is modelled as a voltage source whereas the grid-side converter is modelled as a current source [26,27]. The torque and the speed are controlled by the rotor side converter. The rotor speed is controlled by the q-component of the injected voltage, through rotor side converter. The d-component of the rotor side converter voltage is used for compensation for the generator magnetizing reactive power. The main objective for the grid-side converter is to keep the dc-link voltage constant. In DFIG, the rotor side converter is controlled by using different control techniques such as scalar and vector controls. In scalar control, the torque and flux have a coupling effect while in vector control, the torque and flux has a decoupling effect.

The DFIG equipped with four-quadrant ac-to-ac converter increases the transient stability margin of the electric grids compared to the fixed-speed wind systems based squirrel-cage generators [28]. The stator and the rotor modelling of DFIG are given below:

$$u_{ds} = -R_s i_{ds} - \omega_s \psi_{qs} + \frac{d\psi_{ds}}{dt} \quad (2)$$

$$u_{qs} = -R_s i_{qs} + \omega_s \psi_{ds} + \frac{d\psi_{qs}}{dt} \quad (3)$$

$$u_{dr} = -R_r i_{dr} - s\omega_s \psi_{qr} + \frac{d\psi_{dr}}{dt} \quad (4)$$

$$u_{qr} = -R_r i_{qr} + s\omega_s \psi_{dr} + \frac{d\psi_{qr}}{dt} \quad (5)$$

where s is the slip, u is the voltage, i is the current, R is the resistance, and ψ is the flux, is the synchronous speed of the stator field. All quantities are measured in per unit. The subscripts d and q stand for direct and quadrature component, respectively while subscripts r and s stand for rotor and stator respectively.

The real and reactive power at the rotor and the stator can be calculated by:

$$P_s = u_{ds} i_{ds} + u_{qs} i_{qs} \quad (6)$$

$$Q_s = u_{qs} i_{ds} - u_{ds} i_{qs} \quad (7)$$

$$P_r = (u_{dr} i_{dr} + u_{qr} i_{qr}) \quad (8)$$

$$Q_r = (u_{qr} i_{dr} - u_{dr} i_{qr}) \quad (9)$$

For DFIG

$$P = P_s + P_r = u_{ds} i_{ds} + u_{qs} i_{qs} + u_{dr} i_{dr} + u_{qr} i_{qr} \quad (10)$$

$$Q = Q_s + Q_r = u_{qs} i_{ds} - u_{ds} i_{qs} + u_{qr} i_{dr} - u_{dr} i_{qr} \quad (11)$$

Rotor equations modeling

The general relations between wind speed and aerodynamic torque hold [17]:

$$T_t = \frac{1}{2} \rho \pi R^3 v^2 \frac{C_p(\lambda, \beta)}{\lambda} \quad (12)$$

And the power is shown as

$$P_w = \frac{\rho}{2} C_p(\lambda, \beta) A_R v_w^3 \quad (13)$$

The power coefficient C_p of the wind turbine in equation 13 is a function of tip-speed ratio λ which is given by:

$$\lambda = \frac{\omega R}{v} \quad (14)$$

T_t =turbine aerodynamic torque (Nm), ρ = specific density of air (kg/m³), v = wind speed (m/s), R =radius of the turbine blade (m), C_p = coefficient of power conversion, β = pitch angle, P_w =power extracted from the airflow (W), λ = Tip speed ratio, ω = is the rotational speed of the wind turbine shaft. The value of Q fed into the grid in equation 11 above depends on the control of the power electronic in the grid sides. This does not affect active power except that the efficiency of the inverter can be incorporated into the last two variables. In this paper, the generator is

represented by third order model as indicated in DlgSILENT [20]. In this case the model is obtained by neglecting the stator transients for the fifth order model of induction machine. It shows that there are three electrical equations and one mechanical equation. The model is in d-q expressed in rotor reference frame. In rotor reference frame, the d axis in the rotor reference frame is chosen collinear to the rotor phase winding and the position of the rotor reference frame is the actual position of the rotor.

The dynamic model of the generator is completed by mechanical equation as indicated below:

The electrical torque can be expressed by:

$$T_e = \psi_{dr} i_{qr} - \psi_{qr} i_{dr} \quad (15)$$

Obviously, there is a change in generator speed as a result of the difference in electrical and mechanical torque. This is expressed as:

$$\frac{d\omega}{dt} = \frac{1}{2H} (T_m - T_e) \quad (16)$$

Where H is the inertial constant(s) and this is specified in DlgSILENT as acceleration time constant in the induction generator type. T_m and T_e are the mechanical and electrical torque, respectively.

3.2 Modeling of Small Hydro Turbine

The power available in water current is proportional to the product of head and flow rate [29].

The general formula for any hydro power is:

$$P_{hyd} = \rho gQH \quad (17)$$

Where: P_{hyd} is the mechanical power produced at the turbine shaft (Watts), ρ is the density of water (1000 kg/m^3), g is the acceleration due to gravity (9.81 m/s^2), Q is the water flow rate passing through the turbine (m^3/s), H is the effective pressure head of water across the turbine (m). The hydro-turbine converts the water pressure to mechanical shaft power, which further rotates the generator coupled on the same shaft [30-32]. The relation between the mechanical and the hydraulic powers can be obtained by using hydraulic turbine efficiency η_h , as expressed by the following equations:

$$P_n = \eta_h P_{hyd} \quad (18)$$

$$Q = Av$$

where A is the area of the cross section (m^2) and v is the water flow speed (m/s),

And the whole equation is derived from Bernoulli's theorem which states that:

$$\frac{v^2}{2g} + h + \frac{p}{\rho g} = \frac{P_{hyd}}{\rho gQ} \quad (19)$$

where p is the pressure of water (N/m^2).

3.3 Solar Cell Modeling

Solar PV effect is a basic physical process through which solar energy is converted directly into electrical energy. It consists of many cells connected in series and parallel. The voltage and current output is a nonlinear relationship. It is essential therefore to track the power since the maximum power output of the PV array varies with solar radiation or load current. The equivalent diagram of a solar cell is represented by one diode model as shown in Fig. 4.

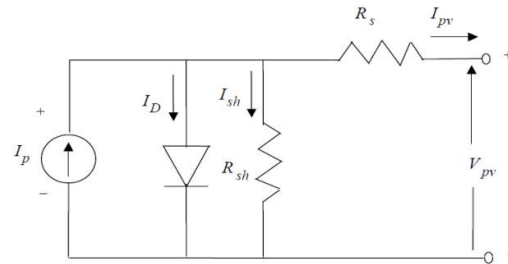


Fig. 4. Model for single solar cell

The output terminal of the circuits is connected to the load. The output current source is the different between the photocurrent I_p and the normal diode current I_D . Ideally the relationship between the output voltage V_{pv} and the load current I_{pv} of a PV cell or a module can be expressed as if we assume that the current I_{sh} in shunt resistor R_{sh} is neglected [33-36].

$$I_{pv} = I_p - I_D = I_p - I_o \left[\exp\left(\frac{V_{pv} + I_{pv}R_s}{mKT_c/q}\right) - 1 \right] \quad (20)$$

where I_p is the photocurrent of the PV cell (in amperes), I_o is the saturation current, I_{pv} is the load current (in amperes), V_{pv} is the PV output voltage (in volts), R_s is the series resistance of the PV cell (in ohms) and m , K and T_c represent respectively the diode quality constant, Boltzmann's constant and temperature. q is electron charge ($1.602 \times 10^{-19} \text{ C}$) [37].

The power output of a solar cell is given by:

$$P_{pv} = V_{pv} I_{pv} \quad (21)$$

Where I_{pv} is the output current of solar cell (A). V_{pv} is the solar cell operating voltage (V), P_{pv} is the output power of solar cell (W). The output power depends on the temperature and the irradiance [38].

3.4 Load Modelling

For dynamic performance analysis, the transient and steady-state variation of the load P and Q with changes in bus voltage and frequency must be modelled. For power system analysis, load can be thought of as real and reactive power launched to lower voltage distribution system at buses. The load can be modelled as: constant real and reactive power, constant current, constant impedance as well as any random combination of the above. Stochastic models possess some inherent randomness. The same set of parameter values and initial conditions will lead to an ensemble of different outputs. Assumption is made that the load has an initial complex power S . The load is modelled as real and reactive power load [39]:

$$S = P + jQ \quad (22)$$

where P and Q are real and reactive power, respectively

4. ARRANGEMENT OF THE PROPOSED CONFIGURATION

Fig. 5 shows the modified single machine infinite bus system modelled in DigSILENT. This power system model consists of an infinite bus system (Grid) represented by GEN1, one centralized generator (GEN2), a hybrid distributed generation (HDG) attached to Bus 2 (not shown) and two equal loads (LOAD1 and LOAD2). GEN1 is connected to bus 3 via line 3. The transmission lines (line 1, line 2 and line 3) are modelled as equivalent π transmission lines. Line 1 and line 2 are 100km long each, while line 3 is 40km long. GEN 2 is connected to bus 2 via a 100MVA transformer (transformer 1) and has a capacity of 80MW and 60MVAR. The DG/HDG consisting of wind generator (DFIG), SOLAR PV and small hydropower system (SHP) is connected to bus 2 via another 100MVA transformer (Transformer 2, not shown in Fig. 5). Each DFIG is rated 8MW, 0.89 power factor

lagging. The SOLAR PV is rated 8MW real power at unity power factor. When SOLAR PV alone is connected to the HDG bus, a capacitor bank is used at that bus to compensate for reactive power. The hydropower is rated 8MW and 4MVAR. LOAD1 and LOAD2 are connected to bus 2 and bus 3, respectively, and are rated 80MW and 40MVAR each. To investigate the effect of a large disturbance, a three-phase fault was applied in the middle of line 2 and cleared after 200 ms by removing the line.

The penetration level in the test system is varied in the following order.

- (i) Import mode, $PL_{HDG} = 40\%$
- (ii) Balanced mode, $PL_{HDG} = 50\%$
- (iii) Export mode, $PL_{HDG} = 80\%$

To combine these three DGs together, an effective truth table was drawn (Table 1) and it can be understood from the inference on column 5. Please note that in Table 1, 0 indicates that the generator was not integrated to the network while 1 indicates that the generator was integrated. For this paper, only scenario 4, 6 and 7 were considered (see Table 1). The transient stability indicator used is critical clearing time and oscillation duration.

4.1 Transient Stability Indicator

The commonly used transient stability index is the critical clearing time. The critical clearing time is the maximum allowable time to maintain synchronism. It measures the robustness of the system to various contingencies. If the fault is clear within this time, the power system remains stable. But if it is cleared after this time, the power system is most likely to loss synchronism. The criterion for instability is when the first swing rotor angle exceeds 120 degrees, otherwise the system is stable. The setting of threshold is always based on power system characteristics. To assess the transient stability of every scenario, we apply a temporary 3-phase fault at the mid-point of line 2 while the load varies and the generation type varies also. The CCT is obtained by increasing the fault duration until GEN 2 loses synchronism at 120 degrees. The second index is rotor angle swinging or oscillation duration. When the CCT is exceeded, the synchronism of the generators can no longer be maintained. The generators will go out of step leading to an increase in rotor angle separation and the generator will refuse to settle.

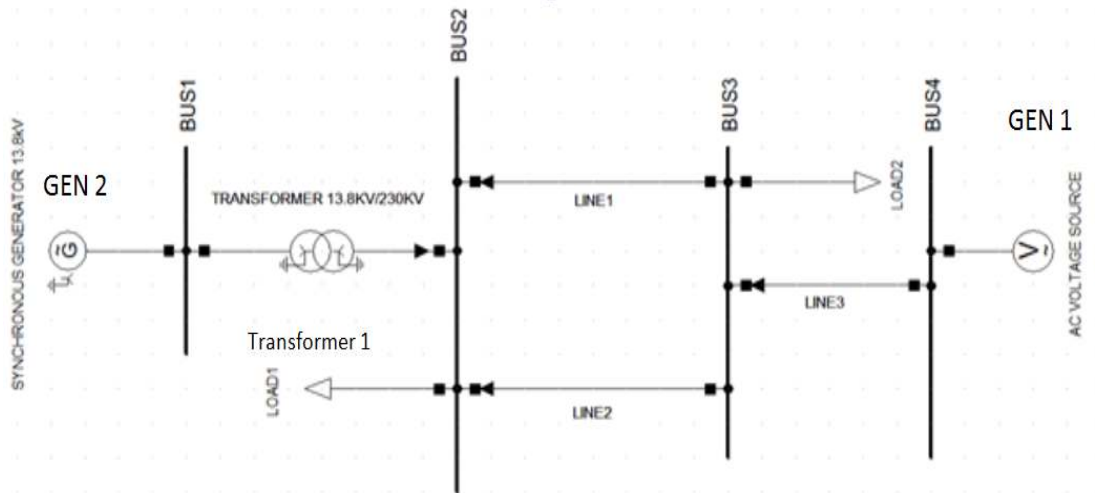


Fig. 5. Arrangement of the proposed configuration in DigSILENT

Table 1. Truth table for hybrid distributed generation

Scenarios	Wind turbine (DFIG)	Solar PV	Small hydropower	Inference
1	0	0	0	No DG Integration
2	0	0	1	Small hydropower only (Base case 1)
3	0	1	0	Solar PV only (Base case 2)
4	0	1	1	Solar PV and Small hydropower
5	1	0	0	Wind Turbine only (Base case 3)
6	1	0	1	DFIG and Small Hydropower
7	1	1	0	DFIG and Solar PV
8	1	1	1	DFIG, Solar PV, and Small Hydropower (SHP)

5. SIMULATION RESULTS WITH VARYING LOAD AND DIFFERENT TYPES OF HDG

In the simulation, the base load is 80MW and 40MVar for each load (LOAD1 and LOAD2). Note that only the export mode is considered. The description of the modelling done in this section explains what happen during the peak load and during the non-peak load. During the peak load, a certain generator will be switched on to cater for the additional load and during non-peak load the generator can be switched off. The particular generator to be switched off or on is being identified in this simulation and modelling.

Table 2. The growth in demand for 30 years with 6 years interval

Years	LOAD (MVA)
0	80 +j40 (base load)
6	104+j52
12	128+j64
18	152+j76
24	176+j88
30	200+j100

The increase in load is covered by using one DG while the other DG covered half of the base load. In other words, after the first 6 years, the increase in load is estimated to be 24+j12MVA. One DG supplied 80+j40MVA (half of base load) while the other DG supplied 24+j12MVA. The

choice of which DG to use to supply the step increase in load demand depends on the availability of the primary source and the location. When DG is used to supply the increasing load, it is assumed that the primary energy source is abundant in such location.

Three assumptions were made:

- 1) Half of the base load was supplied by the SOLAR PV but the increasing load demand was supplied by SHP and vice versa. This is shown in Fig. 6 with the label (SOLAR PV (base load) and SHP (Additional load)).
- 2) Half of the base load was supplied by the SOLAR PV but the increasing load was supplied by the DFIG and vice versa. This is shown in Fig. 7 with the label (SOLAR PV (base load) and DFIG (Additional load)).
- 3) Half of the base load was supplied by the SHP but the increasing load was supplied by the DFIG and vice versa. This is shown in Fig. 8 with the label (SHP (base load) and DFIG (Additional load)).

The first assumption means that the steps increased in the load were supplied by SHP while SOLAR PV supplied half of the total base load and vice versa. Since there are two loads (each $80+j40$ MVA), the total base load is $160+j80$ MVA. While the first load increase is $24+j12$ MVA (reactive power has also increased). Consider the year 30 where the total load is $200+j100$ MVA (see last row in Table 2). The total base load (LOAD1 & LOAD2) is $160+j80$ MVA. The load increase is $120+j60$ MVA for one load.

DG supplies the half of the base load ($80+j40$ MVA) and GEN2 supplies the other part of the base load ($80+j40$ MVA).

6. RESULTS AND DISCUSSION

6.1 Stochastic Load and HDG Penetration Level Impact on Rotor Angle using Oscillation Duration

The graph depicted in Fig. 6 shows that when SOLAR PV supplies the additional load increase ($120+j60$ MVA) and SHP supplies half of the base load, the system has the larger first swing and more subsequent oscillations as compared to when SHP supplies the additional load increase. Also, when SOLAR PV supplies the load increase, which is higher than the base load, the impact of SOLAR PV will be higher or dominant.

When SHP is used to supply additional load increase, the transient stability is improved because SHP can also supply reactive power to the grid.

From Fig. 7 it can be seen that the transient stability margin is decreased when DFIG is used to supply the load increase compared to when SOLAR PV supplies the load increase. This is because in Fig. 7, much of the load is supplied by DFIG which in this paper shows the worst transient stability case. When SOLAR PV is used to supply the load increase in Fig. 7, the stability is improved and the system settled down within 6 seconds.

Fig. 8 shows that the transient stability margin is improved when SHP is used to supply the increasing load and DFIG is used for the base load compared to when DFIG is used to supply the additional load increase.

In all the three graphs (Figs. 6-8), the stability is improved when SHP is used to supply the load increase but worsened when DFIG is used to supply the load increase.

The transient stability depends on the combination of different DGs. For example, the transient stability in Fig. 6 worsened when SOLAR PV supplied the load increase, but in Fig. 7 when SOLAR PV supplied the load increase and DFIG supplied the base load, the stability is improved.

6.2 Stochastic Load and HDG Penetration Level Impact on Critical Clearing Time (CCT)

Consider the last row of Table 3. (i.e., year 30) where the total load is $200+j100$ MVA. Since half of the base load (LOAD 1) is $80+j40$, the load increase is $120+j60$ MVA. Table 3 shows the CCT values during step increase in load demand.

From Table 3, it is observed that the transient stability of the system depends on the DG that is used to supply the highest megawatt (i.e., dominant). For example, in column 2 of Table 3, DFIG is used to supply the additional load while SOLAR PV supplied the base load. When the load was $104+j52$ MVA, DFIG only supplied $24+j12$ MVA, while SOLAR PV is used to supply $80+j40$ MVA. In this case, the impact of SOLAR PV on the transient stability dominates. As the additional load increases, the transient stability margin decreases because the DFIG now supplies the additional load increase and

becomes dominant compared to SOLAR PV. Comparing column 2 with column 3, the transient stability is improved when SOLAR PV supplies the additional loads compared to when DFIG supplies the additional loads (see the average values of the CCT in Table 3, last row).

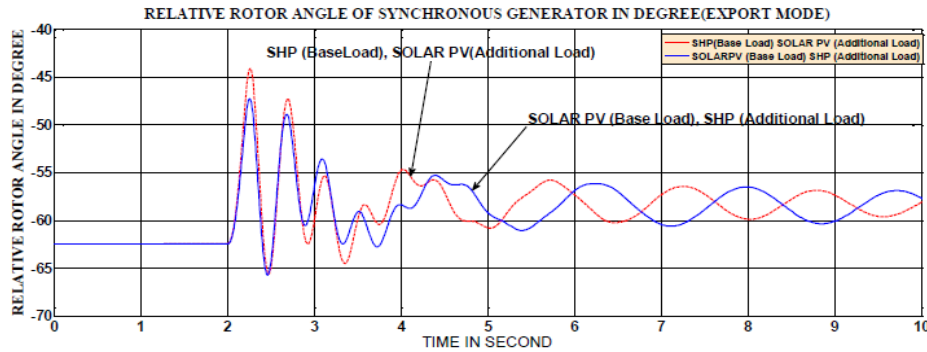


Fig. 6. Rotor angle of (GEN2) indicating Load supply by SOLAR PV and SHP and vice versa (Year 30)

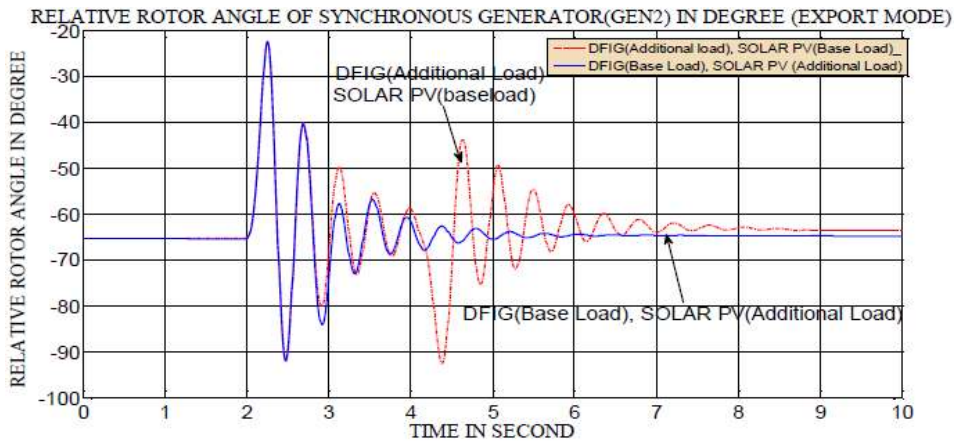


Fig. 7. Rotor angle of (GEN2) indicating Load supply by SOLAR PV and DFIG and vice versa (Year 30)

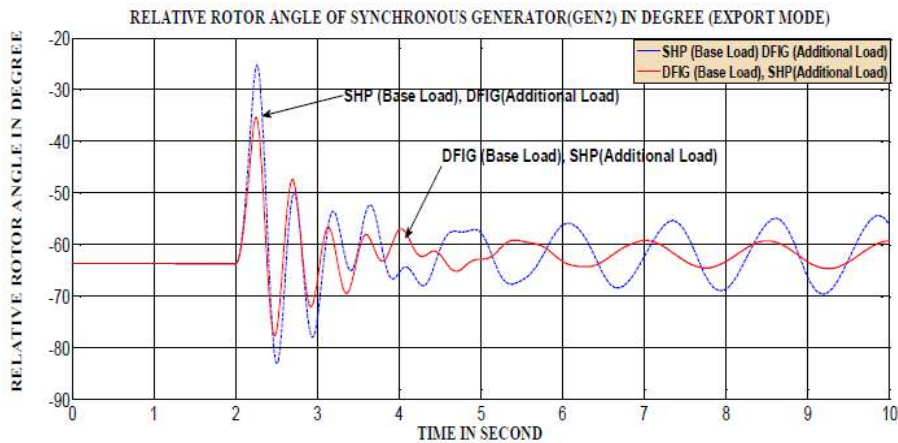


Fig. 8. Rotor angle of GEN 2 indicating load supply by SHP and DFIG and vice versa (Year 30)

Table 3. CCT during step increase in load demand

LOADS (MVA)	DFIG (Additional Load) and SOLAR PV (base load)	DFIG (base load) and SOLAR PV (Additional Load)	SOLAR PV (base load) and SHP (Additional Load)	SOLAR PV (Additional Load) and SHP (base load)	SHP (Additional Load) and DFIG (base load)	SHP (base load) and DFIG (Additional Load)
CCT (ms)						
104+j52	395	310	420	500	400	470
128+j64	380	300	450	490	390	450
152+j76	210	290	470	480	220	140
176+j88	70	130	480	460	120	100
200+j100	65	150	490	450	150	95
Average (ms)						
	224	236	462	476	256	251

It is therefore observed that whenever DFIG supplies the largest megawatt, the transient stability is worsened compared to other DGs.

However, the case of combination of SOLAR PV and SHP is different (columns 4 and 5 in Table 3) take for example when the load is 104+j52. Under this load condition, when SOLAR PV supplies the additional load and SHP supplies the base load (column 5), the transient stability margin is improved compared to when SOLAR PV supplies the based load and SHP supplies the additional load (column 4). This is because SHP initially supplied the highest load (80+j40MVA). But when the load increases and SOLAR PV was used to supply the increasing load, the transient stability margin decreases, but when SHP supplies the increasing load in column 4, the stability margin improves.

However, when SHP supplies the additional load, the transient stability margin was lower initially compared to when SHP supplies the based load (column 5). As more additional loads are added, the transient stability margin continues to increase as can be seen by the increase in the CCT values which increases from 420ms to 490ms. But in column 5, the CCT values decreased. Column 6 shows the CCT when SHP supplies the additional load and DFIG supply the base load while column 7 shows the opposite. It can be seen from the average values of the CCT that the average value of the CCT is lower when SHP is used to supply the base load and DFIG supply the additional load compared to when SHP supplies the additional loads and DFIG is used to supply the base load.

The simulation results indicate that CCT and oscillation duration are good indices that can be used to access the stability of power system under three-phase fault. The level of penetration

and the nature of the load of HDG affect the transient stability of power system.

7. CONCLUSION

Modelling and simulation of grid integrated Hybrid distributed generation as well as the impact of stochastic load and penetration level of HDG on transient stability were investigated in this paper. By observing the oscillation duration and critical clearing time, we were able to assess whether the transient stability of the system was improving or deteriorating. The simulation results show that single source DG and multi-source DG (HDG) will have different impacts on transient stability of power system. Since the generators are better combined together to enhance and to improve power availability, it is necessary to investigate the stability of the system when HDG is integrated. It is shown that transient stability is improved when the combination of HYBRID SOLAR PV+SHP is used compared to when HYBRID DFIG+SOLAR PV is used. However, the transient stability is worsened whenever DFIG is combined with other DGs to supply the additional load compared to when SHP and SOLAR PV are combined. As the additional load increases, the critical clearing time also decreases except in the case of hybrid SOLAR PV (base load) and SHP (additional load).

ACKNOWLEDGEMENT

This work is based on research supported in part by the National research Foundation of South Africa Grant no. 85503.

COMPETING INTERESTS

Authors have declared that no competing interests exist.

REFERENCES

1. Ackerman T, Andersson G, Soder L. Distributed generation, a definition. *Electric Power Energy Research*. 2001;57(3):195-204.
2. Momoh J, Boswell GD. Improving power grid efficiency using distributed generation. *Proceedings of the 7th International Conference on Power System Operation and Planning*. 2007;11-17.
3. Available:<http://www.energy.ca.gov/2007publications/CEC-500-2007-021/CEC-500-2007-021.PDF>
4. Azmy AM. Simulation and management of distributed generation units using intelligent techniques. Ph.D. Thesis Submitted to the Department Electrical Engineering University of Duisburg-Essen; 2005.
5. Olulope PK, Folly KA. Impact of hybrid distributed generation on transient stability of power system. *Power and Energy Systems Applications (PESA 2012)*, Las Vegas, USA, November 12 – 14. 2012;97-105.
6. Olulope PK, Folly KA, Ganesh K, Venayagamoorthy. Modeling and simulation of hybrid distributed generation and its impact on transient stability of power system. *International Conference on Industrial Technology (ICIT)*, 25-27 February; 2013.
7. Paska J, Biczal P, Klos M. Hybrid power systems-An effective way of utilizing primary energy sources. *Electric Power Systems Research*, Elsevier. 2009;1-8.
8. Wang C. Modeling and control of hybrid Wind/photovoltaic/fuel cell distributed generation system. Ph.D Dissertation Submitted to Montana State University; 2006.
9. Thong VV, Driesen J, Belmans R. Transmission system operation concerns with high penetration level of distributed generation. *Universities Power and Engineering Conference UPEC*, 4-6 Sept. 2007;867-871.
10. Tran-Quoc T, Le Thanh L, Ch. Andrieu, Hadsaid N, Kieny C, Sabonnadiere JC, Le K, Devaux O, Chilard O. Stability analysis for the distribution networks with distributed generation. *Proc. 2005/2006 IEEE/PES Transmission & Distribution Conference & Exposition*. Dallas, TX, USA, May 21–26. 2006;(1–3):289–294.
11. Knazkins VV. Stability of power systems with large amounts of distributed generation. PhD Thesis Submitted to University Stockholm, Sweden; 2004.
12. Ishchenko A. Dynamics and stability of distributed networks with dispersed generation. Ph.D Thesis Submitted to Eindhoven University of Technology, 16th January; 2008.
13. Reza M. Stability analysis of transmissions Systems with high penetration of distributed generation. PhD Thesis submitted to Delf University of Technology Delft, The Netherlands; 2006.
14. Tiam Y. Impact on the power system with a large generation of photovoltaic generation. PhD Thesis submitted to the University of Manchester Institute of Science and Technology. 2004;53-55.
15. Vechiu I, Camblong H, Papia G, Dakyo B, Nichita C. Dynamic simulation model of a hybrid power system: Performance analysis. *International Journal of Automotive Technology*. 2006;7(7):1-9.
16. Sotirios S, Papadopoulos B, Demetrios P. Efficient design and simulation of an expandable hybrid (wind-photovoltaic) power system with MPPT and inverter input voltage regulation features in compliance with electric grid requirements. *Electric Power Systems Research*. 2009; 79:1271-85.
17. Mehdi Dali, Jamel Belhadj, Xavier Roboam. Design of a stand- alone hybrid photovoltaic-wind generating system with battery storage. Available:http://journal.esrgroups.org/jes/papers/4_3_7.pdf
18. Joanne Hui, Alireza Bakhshai, Praveen K. Jain. A hybrid wind- solar energy system: A new rectifier stage topology. In: *Applied Power Electronics Conference and Exposition (APEC), 2010 Twenty-Fifth Annual IEEE, 21st – 25th Feb. 2010*;155-61.
19. Arutchelvi Meenakshisundaram, Daniel Samuel Arul. Grid connected hybrid dispersed power generators based on PV array and wind-driven induction generator. *Journal of Electrical Engineering* 2009; 60(6):313-20.
20. Hansen AD, Jauch C, Sørensen P, Iov F, Blaabjerg F. Dynamic wind turbine models in power system simulation tool DigSILENT. *Risø National Laboratory, Roskilde*; 2003.

- Available:www.digsilent.es/tl_files/digsilent/files/powerfactory/application.../ris-r-1400.pdf
21. Freris LL. Wind energy conversion systems. Prentice Hall; 1990.
 22. Sørensen PE, Hansen AD, Janosi L, Bech J, Bak-Jensen B. Simulation of interaction between wind farm and power system. Technical University of Denmark; 2002. Access: orbit.dtu.dk
 23. Nunes MVA, Lopes JAP, Zurn HH, Bezerra UH, Almeida RG. Influence of the variable-speed wind generators in transient stability margin of the conventional generators integrated in electrical grids. IEEE Trans. Energy Convers. 2004;19(4):692–701.
 24. Morren J, de Haan SWH. Ridethrough of wind turbines with doubly-fed induction generator during a voltage dip. IEEE Trans. Energy Convers. 2005;20(2):435–441.
 25. Ekanayake JB, Holdsworth L, Wu X, Jenkins N. Dynamic modeling of doubly fed induction generator wind turbines. IEEE Trans. Power Syst. 2003; 18(2):803–809.
 26. Poller MA. Doubly-fed induction machine models for stability, assessment of wind farms. In Power Tech Conference Proceedings 2003 IEEE Bologna. 2003;3: 6.
 27. Qiao W. Dynamic modeling and control of doubly fed induction generators driven by wind turbines. In Power Systems Conference and Exposition, 2009. PSCE '09. IEEE/PES. 2009;1–8.
 28. Gautam D, Vittal V, Harbour T. Impact of increased penetration of DFIG based wind turbine generators on transient and small signal stability of power systems. In 2010 IEEE Power and Energy Society General Meeting. 2010;1.
 29. Dolf Gielen. Renewable energy technologies; Cost analysis series. IRENA International Renewable Energy Agency; 2012.
 30. Ramos H. Guidelines for design of small hydropower plants; 1999.
 31. Small hydropower systems, U.S. Department of Energy (DOE) by the National Renewable Energy Laboratory (NREL); 2001.
 32. Hydropower basics. Available:<http://www.microhydropower.net/basics/turbines.php>
 33. Ye L, Sun HB, Song XR, Li LC. Dynamic modeling of a hybrid wind/solar/hydro microgrid in EMTP/ATP. Renew. Energy. 2012;39(1):96–106.
 34. Mukund R. Patel. Wind and solar power systems. United States of America: CRC Press; 1999.
 35. Gray L. The physics of the solar cell A. Luque, S. Hegedus (Eds.), Handbook of Photovoltaic Science and Engineering, Wiley, New York. 2003;(Chapter 3):61–111.
 36. Chenni R, Makhlof M, Kerbache T, Bouzid A. A detailed modeling method for photovoltaic cells. Energy. 2007;32(9): 1724–1730.
 37. Ramos Hernanz, et al. Modelling of photovoltaic module. International Conference on Renewable Energies and Power Quality ICREPQ'10 Granada (Spain), 23th to 25th March; 2010.
 38. De Blas M, Torres J, Prieto E, Garcia A. Selecting a suitable model for characterizing photovoltaic devices. Renew. Energy. 2002;25(3):371–380.
 39. Kepka J. Load modeling for power system analysis. Poland: Wroclaw University of Technology. 2014;1–4. Available: eeeic.org/proc/papers/111.pdf

© 2016 Olulope and Folly; This is an Open Access article distributed under the terms of the Creative Commons Attribution License (<http://creativecommons.org/licenses/by/4.0>), which permits unrestricted use, distribution, and reproduction in any medium, provided the original work is properly cited.

Peer-review history:
The peer review history for this paper can be accessed here:
<http://sciencedomain.org/review-history/17297>